Integrated landscape genomics reveals biogeography and climate-driven local adaptation in high-altitudes

Nan Wang[1,#,], Prashant Ghimire[2,#,*], Pritam Chhetri[3], Nishma Dahal[3], Cheng Yi[1], Tong Zhang[4], Suonan Zhuoga[5], Zhaxi Jiangyong[5], and Sangeet Lamichhaney[2,6,*]*

[1]School of Ecology and Nature Conservation, Beijing Forestry University, Beijing 100083, P. R. China.

[2]Department of Biological Sciences, Kent State University, Kent 44240, USA.

[3]Biotechnology Division, CSIR-Institute of Himalayan Bioresource Technology, Palampur, HP, 176061, India.

[4]Central South Inventory and Planning Institute of National Forestry and Grassland Administration, Changsha, 410014, China.

[5]Forestry and Grassland Bureau of Yusu, Qinghai, 815099, China.

[6]School of Biomedical Sciences, Kent State University, Kent, OH 44240, USA.

[#]Wang and Ghimire contributed equally to this work.

[*]Corresponding authors: Nan Wang (wangnan761227@bjfu.edu.cn), Prashant Ghimire (pghimir1@kent.edu), and Sangeet Lamichhaney (slamichh@kent.edu).

Abstract

High-elevation environments harbor unique species adapted to altitudinal and environmental extremes. However, due to logistical challenges of sampling such species throughout their distribution across steep and varied terrains, studies often lack comprehensive evidence to understand patterns of population divergence, local adaptation, and how current adaptations may influence future vulnerability. In this study, we utilized Tibetan Partridge *(Perdix hodgsoniae)*, a high-altitude endemic bird found between 2800–5000 meters across the arid western and humid northeastern regions of the Sino-Himalayan landscape. This region's complex topography-characterized by tall mountains, deep valleys, and contrasting climatic conditions provided opportunities for investigating population divergence, local adaptation, and climate-related vulnerability. We integrated population-scale whole-genome sequencing with ecological, climatic, landscape, and morphological data to examine current patterns of local adaptation and forecast future risks. Our findings show that both biogeographic barriers and climatic variation drive rapid population divergence in *P. hodgsoniae*, reflected in distinct morphological traits and population genetic structure. Western populations, inhabiting dry and fragmented landscapes, exhibit adaptations to temperature extremes with low genetic diversity, reduced habitat suitability, limited gene flow, and weak connectivity—factors that increase their vulnerability to future environmental changes. In contrast, northeastern populations, living in more humid regions, show genetic adaptations linked to precipitation, maintain high genetic diversity and habitat connectivity, and may serve as evolutionary refugia under future climate scenarios. This study underscores the value of integrating genomic, ecological, and landscape data to reveal mechanisms of divergence and adaptation, and to develop robust predictions for conservation planning under rapidly changing environmental conditions.

Keywords: High altitude, local adaptation, Climate, Biogeography, Tibetan Partridge, Sino-Himalaya.

Introduction

Mountains are unique ecosystems shaped by complex geological processes. The formation of mountains, deep valleys, rivers, and drainage systems has driven biodiversity diversification. As a result, mountains host approximately 87% of the world's terrestrial biodiversity within just 25% of the landmass (Colwell et al. 2008; Rahbek et al. 2019). However, these ecosystems are among the most vulnerable to climate change(Knight 2022). Extensive research has been conducted on mountain ecosystems to understand biodiversity patterns (Peters et al. 2019; Rahbek et al. 2019; Hu et al. 2020). Such studies have indicated that geological events, such as plate tectonics and climatic oscillations, including glacial cycles, have left significant imprints on mountain biodiversity (Descombes et al. 2017; Hu et al. 2020). Our current understanding of mountain ecosystems largely comes from broad community-level studies examining changes in species richness, abundance, and diversity along elevational gradients. These studies have demonstrated that many species are shifting toward higher elevations in response to climate change (Freeman et al. 2018; Rödder et al. 2021). However, much less is known about species that already inhabit mountain summits, particularly the endemic species.

High-altitude endemic species are particularly vulnerable to environmental change, as they already face physiological challenges from low oxygen availability and atmospheric pressure (Laguë 2017; Storz 2021). Unlike lowland species that can track their favorable niches by moving upslope in response to changing environment, species confined at the top have limited flexibility to track their favorable niches and hence, face severe constraints (Freeman et al. 2018; Rödder et al. 2021). Their range expansion is restricted not only by existing geographical barriers but also by the stark climatic contrasts within mountain landscapes (Sánchez-Montes et al. 2018). This raises critical questions: How do these species persist in complex biogeographic regions with fragmented habitats and variable environmental conditions? Are their responses to environmental changes uniform across their habitat distribution, or do local biogeography and environmental factors drive distinct adaptive strategies? Additionally, do certain local populations exhibit greater vulnerability due to variations in biogeographic constraints and their genomic architecture?

Addressing these questions requires a comprehensive study of the local populations of such high-altitude endemic species across their distributional range, encompassing diverse landscape and climatic gradients. By integrating landscape and climatic data with population-scale genomic data, we can gain deeper insights into how populations respond to different climatic pressures across their range and identify genetic signatures of local adaptation. Additionally, integrating landscape genomics and eco-evolutionary modeling approaches will allow prediction of "genomic offset", a measure of the genetic changes required for a local population to adapt to future environmental changes (Rellstab et al. 2021; Chen et al. 2022). Such a comprehensive framework will allow us to accurately identify vulnerable populations and landscapes, enhancing our ability to develop targeted conservation strategies (Bay et al. 2018; Turbek et al. 2023).

The species residing in the Sino-Himalayan region, encompassing the Himalayas and the Qinghai-Tibetan Plateau can offer one such framework to study how species persist in fragmented landscapes and how their genetic adaptations may influence their future survival in a rapidly changing environment. The region's intricate topography, shaped by the continuous collision of the Indian and Eurasian tectonic plates over the past 50 million years, along with past and ongoing climatic fluctuations, has created substantial biogeographic barriers, including mountain ranges, deep valleys, and expansive plateaus, driving species isolation and diversification (Favre et al. 2015). Recognized as a biodiversity hotspot, this region harbors numerous endemic flora and fauna uniquely adapted to extreme high-altitude environments.

Studying endemic species in the Sino-Himalayan region not only offers insights into historical evolutionary processes but also helps us understand how organisms adapt to ongoing climate change in extreme environments. One such high-altitude endemic species is the Tibetan partridge (*Perdix hodgsoniae*), which inhabits montane shrublands at elevations ranging from 2,800 to 4,600 meters(McGowan and Madge 2010) (Fig. 1a). Although capable of short flights, *P. hodgsoniae* primarily relies on walking, making it largely sedentary with minimal altitudinal migration (Lu and Ciren 2002). This limited mobility, combined with their geographic isolation, results in the formation of multiple local populations across their range.

The western portion of its range, bordered by the Himalayas to the south, the Gangdis Mountains to the north, and the Nianqing Tanggula Mountains in the central east, experiences lower

precipitation(Favre et al. 2015) (Fig. 1a, b). In contrast, areas east of the Nianqing Tanggula Mountains, characterized by mid-elevation valleys, receive higher precipitation (Fig. 1a, b). The species' northern distribution is limited by the Qilian Mountains, with the Yellow River and its tributary, the Huangshui River, forming a natural boundary separating it from the Hengduan Mountains **(Fig. 1a).** Given the substantial variation in precipitation across its distribution range, we hypothesize that precipitation exerts a stronger influence than temperature on local adaptation in Tibetan Partridge populations **(Fig. 1b,c)**. We predict to identify genomic signatures of selection associated with precipitation-related variables, reflecting the orographic effects that drive environmental heterogeneity. Populations in wetter north-eastern regions and drier western regions may exhibit distinct genetic adaptations corresponding to their respective climatic conditions.

In this study, we have developed Tibetan Partridge as a model for understanding how animals with ranges spanning diverse high-altitude habitats may respond to current and future environmental changes. In addition, we have highlighted how integrated analysis of landscape, genomic and climate data can provide a comprehensive understanding of which populations may be more resilient or vulnerable, helping to inform conservation strategies for any species facing global change. We have quantified the patterns of biogeography and climate of the Sino-Himalayan landscape and quantified their impact on divergence and species' responses to environmental changes. We have further employed ecological and landscape genomics approaches to identify populations that are at greater risk from climate change and map potential gene flow routes that could facilitate their evolutionary rescue.

Results and Discussion

Geography and historic isolation shape morphology and population genetic structure in Tibetan Partridges: We measured nine morphological traits from 60 Tibetan partridge individuals sampled across their distribution range in the Qinghai-Tibet Plateau (QTP) region of the Sino-Himalayas (see methods for details). Our analysis revealed notable morphological variation among local populations of Tibetan partridge. Beak, paw, and tarsometatarsus length were significantly different across landscapes ($p < 0.05$), with larger size in the north-eastern

143 populations (from Hengduanshan and Qilian landscapes), while wing and tail length showed
144 little variation across the landscape but tended to increase from the western (from Western and
145 Yarlung Zangbo landscapes) to the northeastern regions **(Fig. 2a, Supplementary Fig. 1a-h).** To
146 determine whether the morphological traits exhibited distinct patterns across each landscape, we
147 performed a principal component analysis (PCA) on these nine morphological traits that revealed
148 a clear separation between the western and north-eastern populations, indicating morphological
149 differences among local populations of Tibetan Partridges residing in these different habitats
150 **(Fig. 2b)**. Our morphological analysis indicates that Tibetan partridge populations in dry
151 landscapes tend to have smaller body sizes compared to those in wetter environments. This
152 difference likely reflects the landscape features such as mid-elevational region on wet
153 Hengduanshan, and birds' reliance on shrubland for food, which is relatively sparse in the drier
154 western regions **(Fig. 1c, Supplementary Fig. 2a,b)**, and smaller body size offering an adaptive
155 advantage in these resource-limited conditions. In contrast, in wetter regions with abundant
156 vegetation and more readily available food resources, a larger body size may enhance the birds'
157 ability to efficiently access and store these resources.
158
159 We further conducted whole-genome sequencing of 96 individuals of Tibetan Partridges at ~20-
160 25X average sequence coverage for each sample **(Supplementary Fig. 3)** from 28 different
161 locations across these four landscapes **(Fig. 1a)** and 10 individuals from two closely related
162 species residing at lower elevations; Daurian Partridge *(P. dauurica)* and Grey Partridge *(P.*
163 *perdix)*. We used this genomic data to generate ~5.1 million high-quality SNPs that were
164 polymorphic in at least one population. A maximum likelihood phylogenetic tree based on these
165 SNPs identified that populations from each of the four landscapes in western (Western and
166 Yarlung Zangbo) and north-eastern (Hengduanshan and Qilianshan) region formed genetically
167 distinct clades (**Fig. 2c)**. We estimated that the divergence of Tibetan partridge populations
168 occurred between 0.33 (0.35) and 0.05 (0.004) million years ago (mya) **(Supplementary Fig.**
169 **4a)**. The initial divergence took place between the western and north-eastern populations around
170 0.33-0.35 mya, followed by the split of the Nanjiang Basin population from the Qilianshan and
171 Hengduanshan populations in the north-east approximately 0.09-0.11 mya. A subsequent
172 divergence occurred within a similar timeframe (~0.05-0.07 mya), separating the Qilianshan and
173 Hengduanshan populations. Principal component analysis (PCA) using 291,338 Linkage-

Disequilibrium (LD)-pruned SNPs revealed clustering patterns consistent with the phylogenetic tree, clearly separating populations from the western and northeastern landscapes **(Fig. 2d).** These results indicated that the population divergence of Tibetan Partridge across their distribution range in the Sino-Himalayan landscape is strongly influenced by the region's mountain ranges and river basins, highlighting the significant role of geography in shaping their genetic divergence.

Admixture analysis revealed distinct population structures at (a) both the western and north-eastern edges of the distribution, (b) in the low-elevation population (2,900 m) within the Yarlung Zangbo landscape and (c) populations from the Hengduanshan landscape **(Fig. 2e)**. In contrast, other populations from the Yarlung Zangbo and Qilianshan landscapes displayed relatively high levels of admixture, suggesting greater gene flow among the populations within these regions. We also employed Estimated Effective Migration Surfaces (EEMS) analysis (Petkova et al. 2016) to map corridors and barriers to gene flow across these landscapes. EEMs analysis identified the Nianqing Tanggula mountains, separating the habitats of western and north-eastern populations, as a potential barrier to gene flow **(Fig. 2f).** It also indicated that high elevation areas at the upper stretches of the Yarlung Zangbo region and north of the Yellow River could act as a barrier to gene flow. Consistent with the results from admixture analysis **(Fig. 2e)**, EEMS highlighted possible gene flow corridors within the Yarlung Zangbo landscape. Additionally, the Hengduanshan region displayed both areas (a) supporting lower gene flow (on the northeast and eastern edges) and (b) regions supporting higher gene flow (to the west and east of the Yellow River) **(Fig. 2f)**. To further characterize the patterns of genetic variation across the distribution range of Tibetan partridges, we used Multiple Regression on Distance Matrices (MRM) to assess the relative contributions of geographic distance (Isolation by Distance, IBD) and environmental differences (Isolation by Environment, IBE) to genetic differentiation (FST). Our analysis revealed that environmental distance ($\beta = 0.0771$, $p = 0.001$) has a stronger influence on genetic variation compared to geographic distance ($\beta = 0.0000433$, $p = 0.125$), which was not statistically significant. The full model explained 38.1% of the genetic variation ($R^2 = 0.381$, $p = 0.001$), indicating that environmental factors (IBE only, $R^2 = 0.362$, $p = 0.001$) play a more prominent role than geographic distance (IBD only, $R^2 = 0.147$, $p = 0.002$) in shaping the genetic structure of Tibetan partridges. **(Supplementary Fig. 4b,c)**.

205 Phylogenetic dating, admixture, and EEMS analyses indicate that the biogeographic history of
206 the Tibetan Partridge has been shaped by three major geographic barriers, resulting in the
207 formation of genetically distinct local populations. The primary barrier is the Nianqing Tanggula
208 Mountains, which separated western and northeastern populations approximately 0.35 million
209 years ago. Subsequently, the Yellow River isolated the Hengduanshan population around 0.06
210 million years ago, while high-elevation zones along the upper Yarlung Zangbo River further
211 separated the western and Yarlung Zangbo populations approximately 0.06 million years ago. It
212 is unlikely that these divergence events were driven by the uplift of the Qinghai-Tibetan Plateau
213 (QTP), as the region had already reached its current altitude by the late Pliocene (2.58 million
214 years ago) (Wang et al. 2014; Deng and Ding 2015). Instead, similar to the populations of Snow
215 Partridge, which is previously known to diverged during the same period (~0.4 million years
216 ago) in QTP (Yao et al. 2022), early divergence in Tibetan Partridges may have also been
217 influenced by interglacial isolation. Notably, the latter two divergence events occurred almost
218 simultaneously during Marine Isotope Stage (MIS) 3 (0.06–0.03 million years ago), a period of
219 extensive glaciation in the QTP that caused significant climatic fluctuations(Owen et al. 2003;
220 Cui et al. 2018). While previous studies have highlighted the role of the Nianqing Tanggula
221 Mountains in shaping the west and north-east divergence of diverse species in the Sino-
222 Himalayan region(Liu et al. 2018; Du et al. 2020; Rana et al. 2021), the impact of high-elevation
223 zones in the upper stretches of the Yarlung Zangbo and the Yellow River had remained largely
224 unexplored. Earlier studies from thisin this region were constrained by limited sampling across
225 species distribution range (especially from Tibet)(Du et al. 2020; Chen et al. 2022; Chen et al.
226 2023; Jiao et al. 2024). This study presents a comprehensive sampling of Tibetan partridges
227 across these regions, offering new insights into their biogeographic history and the influence of
228 diverse landscapes on population divergence.

229 **Tibetan partridge populations demonstrate genetic adaptation to local climatic conditions:**
230 Climatic variation in the Sino-Himalayan landscape has led to the population divergence of
231 many species in the region(Yao et al. 2022). There is a considerable variation in temperature and
232 precipitation across different landscapes **(Fig. 1b,c)**, driven by the region's complex topography,
233 characterized by tall mountain ranges and diverse altitudinal gradients. We expect these
234 differences in bioclimatic variables are crucial for shaping the ecological dynamics, habitat

suitability, and adaptive strategies of local Tibetan Partridge populations residing across these varied landscapes. Our comprehensive sampling of the local populations of Tibetan partridges across diverse landscapes within the Sino-Himalayan region provided a unique opportunity to study their adaptation to varying local climatic conditions. To identify key bioclimatic variables for Genotype-Environment Association (GEA) analysis, we ranked the importance of all 19 bioclimatic variables available in the WorldClim database from this region (Fick and Hijmans 2017) using the gradientForest analysis (Ellis et al. 2012). Additionally, we calculated pairwise correlations between these variables to ensure the selection of independent bioclimatic variables. From this analysis, we selected five key variables (BIO2, BIO8, BIO9, BIO12, and BIO15) that ranked high in importance, showed low correlation ($|r| < 0.6$), and represented both temperature and precipitation-related variables **(Supplementary Fig. 5, Supplementary Table 1).**

To identify genomic variants associated with the selected bioclimatic variables, we employed two distinct approaches to minimize false positives. First, we used the Latent Factor Mixed Model (LFMM) (Frichot et al. 2013) to examine univariate relationships between SNPs and each bioclimatic variable. The LFMM analysis identified 442,926 candidate SNPs associated with these five bioclimatic variables after adjusting for multiple testing using FDR correction ($p < 0.05$) **(Fig. 3a, c & Supplementary Fig. 6a-c).** Candidate SNPs associated with specific bioclimatic variables are expected to exhibit significant allele frequency differences among individuals residing across these climatic gradients. To evaluate this, we calculated pairwise genetic divergence (F_{ST}) between 10 individuals from habitats with the highest and lowest values for these bioclimatic variables. The analysis confirmed that the candidate SNPs showed significantly greater genetic differences compared to an equal number of randomly selected SNPs **(Supplementary Fig. 7a-e)**, aligning with our prediction. Most (94.96%) of the candidate SNPs identified by LFMM univariate analysis were associated with precipitation-related variables (BIO12 and BIO15), whereas only relatively smaller proportions (5.04%)) were associated with temperature-related variables (BIO2, BIO8, and BIO9) **(Supplementary Fig. 8)**. These results support our hypothesis that precipitation plays a stronger role than temperature in driving local adaptation in Tibetan Partridge populations.

The second approach we used for GEA analysis was multivariate redundancy analysis (RDA) (Capblancq and Forester 2021) to identify genomic regions associated with previously selected five bioclimatic variables (BIO2, BIO8, BIO9, BIO12, and BIO15). The first three RDA components explained, respectively, 66.76%, 17.47% and 6.18% of the variation. The results showed that individuals residing in the same landscapes clustered together, indicating exposure to similar climatic conditions within each landscape **(Fig. 3e,f)**. Both RDA plots, RDA1 vs. RDA2 **(Fig. 3e)** and RDA1 vs. RDA3 **(Fig. 3f)** revealed that genetic variation in individuals from Hengduanshan and Qilianshan landscapes are positively related with high Annual Precipitation (BIO12) and Precipitation Seasonality (BIO15). In contrast, genetic variation in individuals from the Western and Yarlung Zangbo landscapes are positively related with Mean Diurnal Range (BIO2), Mean Temperature of Wettest Quarter (BIO8), and Mean Temperature of Driest Quarter (BIO9), demonstrating varying climatic associations between the western and north-eastern populations of Tibetan partridges. These results, indicate distinct climatic associations among Tibetan Partridge populations across their distribution range, aligning with our hypothesis. While precipitation-related variables predominantly drive genetic variation in the northeastern populations, temperature plays a more significant role in shaping genetic variation in the Yarlung Zangbo and western landscapes. In dry regions, species must adapt to extreme heat and limited water availability, making temperature regulation crucial for survival (Fuller et al. 2021). Conversely, in wetter north-eastern regions, adaptation to high moisture levels and excessive precipitation is the key. These findings underscore how diverse environmental factors across heterogeneous landscapes drive divergent evolutionary responses, shaping local adaptations in Tibetan Partridges.

We further performed outlier detection using redundancy analysis and identified 14,999 candidate SNPs (0 SNPs RDA1, 164 SNPs RDA2, 14835 SNPs at 3.5 SD) associated with these five bioclimatic variables (BIO2, BIO8, BIO9, BIO12, and BIO15). RDA1 is most strongly associated with BIO12 (Annual Precipitation; loading = -0.67) and BIO9 (Mean Temperature of Driest Quarter; loading = 0.58), while RDA2 is primarily driven by BIO8 (Mean Temperature of Wettest Quarter; loading = 0.78) and BIO12 (loading = 0.70). RDA3 shows moderate associations with BIO2 (Mean Diurnal Range; loading = 0.25) and BIO8 (loading = -0.49), though with weaker overall correlations. Of these, 4,377 candidate SNPs were detected by both

296 the univariate (LFMM) and multivariate (RDA) analyses **(Supplementary Fig. 8)**. We defined
297 these overlapping 4,377 SNPs as "climate-associated core candidate SNPs" and were selected for
298 downstream functional annotation and enrichment analysis. One of the top candidate SNPs
299 associated with BIO9 (Mean Temperature of the Driest Quarter) (Scaffold_631:373,769, A/C,
300 $p < 0.05$) overlaps with the *Store-operated calcium entry-associated regulatory factor (SARAF)*
301 gene. This SNP shows a higher frequency of the A allele in the regions with high mean
302 temperatures **(Fig. 3b)**. *SARAF* activates the mechanistic target of the Rapamycin (mTOR1)
303 pathway, which is linked to heat stress and impacts signal transduction in avian skeletal muscle
304 (Sanlialp et al. 2020). Similarly, another top candidate SNP associated with BIO12 (Annual
305 Precipitation) (Scaffold_720:849,107, T/C, $p < 0.05$) overlaps with the *Tropomodulin-1*
306 *(TMOD1)* gene. This SNP demonstrates near fixation of two alleles in the regions characterized
307 by either dry or wet conditions, highlighting distinct allele frequencies in local populations
308 residing in habitats with varying precipitation levels **(Fig. 3d)**. *TMOD1* which is critical for
309 cellular stability and cytoskeletal organization (Yamashiro et al. 2012), may play a role in
310 cellular responses to osmotic stresses, such as varying precipitation levels.
311
312 The majority of these climate-associated core candidate SNPs were non-coding (n = 4,313,
313 98.5%), and only 64 (1.5%) were coding SNPs **(Supplementary Table 2).** We further extracted
314 295 genes within the 100 kb region upstream and downstream from these SNPs (to extract their
315 potential regulatory regions) and annotated their Gene Ontology and associated metabolic
316 pathways (**Supplementary Resource 1).** Enrichment analysis of these genes identified
317 significant enrichment of three Gene Ontology terms; Adult behavior (*GO:0030534*, p-value=3.9
318 x 10^{-6}), neurotransmitter receptor internalization (*GO:0099590*, p-value=1.7 x 10^{-05}) and
319 diacylglycerol kinase activity (*GO:0004143*, p-value=1.9 x 10^{-05}). In addition, we identified 27
320 missense mutations among these 4,377 "climate-associated core candidate SNPs" spanning 22
321 genes (**Supplementary Resource 2)**. Although no significant pathway enrichment was detected,
322 these genes include notable examples linked to adaptation to precipitation and temperature. For
323 instance, the *Ras and Rab Interactor 2 (RIN2)* gene is associated with plastic responses to dry
324 environments (Kordonowy and MacManes 2017), while the *Epidermal Growth Factor Receptor*
325 *(EGFR)* and *Ecto-NOX Disulfide-Thiol Exchanger 2 (ENOX2)* genes are known for their roles in
326 responding to heat stress (Kaushik et al. 2016; Wang et al. 2022). These results indicate that

327 multiple genes and regulatory pathways associated with response to environmental stimuli
328 (Verburg-van Kemenade et al. 2017; Stonehouse et al. 2024) contribute to the climate-driven
329 local adaptation in Tibetan Partridges.
330
331 **Genomic offsets and niche modeling reveal vulnerable Tibetan partridge populations**
332 **across the Sino-Himalayan landscape:** The heterogeneous landscape of the Sino-Himalayan
333 region includes diverse environmental and topographical conditions **(Fig. 1b,c, Supplementary**
334 **Fig. 2a,b)**, which expose local populations of Tibetan Partridges to varying levels of
335 vulnerability to short and long-term environmental changes. We calculated genomic offsets using
336 4,377 climate-associated core candidate SNPs among the local populations of Tibetan Partridge
337 across their distribution range. Genomic offset measures the genetic distance between current
338 and future genomic compositions, with the latter predicted based on current genotype-
339 environment relationships (Rellstab et al. 2021). A higher genomic offset indicates a greater
340 challenge for a local population to adapt to future climatic scenarios and become more
341 vulnerable to future environmental changes. We employed Gradient Forest (GF) analysis to
342 estimate genomic offset by modeling allele frequency changes along the environmental gradients
343 (Ellis et al. 2012). GF analysis predicted an increase in genomic offset over time (2070 to 2090)
344 and under more extreme climatic conditions **(Supplementary Fig. 9a-c)** among the local
345 populations**.** At the landscape scale, higher genomic offsets were predicted at the edges of the
346 Tibetan partridge's distribution range **(Fig. 4a-b, Supplementary Fig. 9a-c).** The western
347 landscape showed the highest genomic offset, followed by Qilianshan, and Yarlung Zangbo, and
348 the lowest genomic offset was predicted for the Hengduanshan landscape.
349
350 In addition to the population-scale genomic data, we also utilized the current distribution of the
351 Tibetan partridge to quantify its present niche and predict future changes in the Sino-Himalayan
352 landscape. We downloaded, and cleaned the distribution data of Tibetan Partridge from GBIF
353 (https://www.gbif.org/) and performed ecological niche modeling using biomod2 (Thuiller et al.
354 2016). We combined the IUCN range map, and GBIF distribution data to delineate the
355 distribution area of Tibetan partridge. Based on the distinct genetic clustering of the local
356 Tibetan Partridge populations **(Fig. 2)** and the variable climatic environment they are exposed to
357 **(Fig. 1)**, we modeled separately for two landscapes (western and north-eastern). Niche modeling

analysis revealed significant variation in the bioclimatic variables that determined the suitability of habitats for Tibetan partridge populations across different landscapes **(Supplementary Table 3)**. In the western landscape, five bioclimatic variables; three related to temperature (BIO2, BIO4, BIO8) and two related to precipitation (BIO15, BIO19) had higher variable importance and therefore were important predictors of niche suitability **(Supplementary Table 3).** In contrast, in the north-eastern landscape, only three variables (BIO5; related to temperature, and BIO15/BIO14; related to precipitation) had higher variable importance, indicating diverse responses of different populations to their local climatic conditions.

Niche modeling analysis also revealed that 38.9% of the current habitat of Tibetan partridges is suitable, with the Hengduanshan landscape containing the largest proportion of suitable area (15.1%), followed by Yarlung Zangbo (12.05%) while the western (6.1%) and Qilianshan (5.6%) regions have the lowest suitability **(Fig. 4c, d).** This result indicate that there is differences in total suitable areas among landscapes in line with known pattern that species niche suitability declines towards the extreme of their distribution(Brown 1984). Under future projected climate change scenarios, the proportion of suitable areas significantly decreases across all landscapes **(Fig. 4d)**. Dry regions, particularly in the western landscape and outer areas of the Qilianshan landscape, were predicted to experience a significant decline in habitat suitability for Tibetan partridges. To assess the connectivity of the landscape for the potential movement of a species across its distribution range, we further used a simplified approach that combines the habitat suitability index with landscape variables such as elevation, elevation variability, and slope to create a resistance surface (Chen et al. 2022) (see method for details). Consistent with our EEMS findings **(Fig. 2f),** high resistance to species movement was observed across the Nianqing Tanggula mountains **(Fig. 4e)**, indicating limited dispersal ability between populations in western and north-eastern regions. Increased resistance was also identified along the edges of the Western and Yarlung Zangbo landscapes. In contrast, the Hengduanshan landscape displayed greater connectivity both within its area and with the Qilianshan landscape, suggesting stronger connectivity across northeastern landscapes.

These results indicated that Tibetan Partridge populations in the Western landscape, where suitable habitat constitutes only a small proportion (~6%), exhibit the highest genomic offset.

Expansive desert areas and the complex topography characterized by tall mountains in this region limits their ability to migrate toward the more suitable Hengduanshan landscape. Additionally, we observed low genetic diversity within these populations **(Fig. 4f)**, suggesting reduced genetic variation, which may limit their evolutionary flexibility and increase their vulnerability to changing environmental conditions. This pattern aligns with findings in isolated populations in other species that struggle to adapt to future environmental changes(Ruegg et al. 2018). Our findings are also consistent with previous studies on mammals, birds and plants in this region (Du et al. 2020; Chen et al. 2022; Chen et al. 2023; Jiao et al. 2024), which highlight how high-elevation mountains obstruct humid air, create drier conditions, restrict gene flow, and drive population divergence.

The Tibetan Partridge population in the Qilianshan landscape, located at the north-eastern edge of its range, shows a moderate genomic offset and limited proportion of suitable habitat (~5%), identifying them as another potentially vulnerable populations. However, unlike the Western populations, this group may benefit from relatively better landscape connectivity and mid-elevation corridors, which could facilitate migration toward the more favorable Hengduanshan region. Additionally, the Qilanshan population also demonstrates higher genetic variation and admixture with the Hengduanshan population, suggesting greater genetic diversity could enhance its adaptability to environmental shifts. In contrast, the Yarlung Zangbo population, while sharing lower genetic variation and a moderate genomic offset with the Western population, benefits from a relatively higher proportion of suitable habitat (~12%). Notably, this region harbors the lowest elevation Tibetan Partridge population at 2,900 meters, which diverged approximately 150,000 years ago during the Ghonge movement (Palacios et al. 2023). We believe this population has expanded its elevational niche, showcasing adaptations to diverse environmental conditions despite genetic constraints.

The Hengduanshan region, characterized by its complex terrain of intersecting mountain ranges and rivers, along with a diverse altitudinal range, fosters a diverse climatic environment. The local population of Tibetan Partridge from this region stands out for its high genetic diversity, a lower genomic offset, and a significant proportion of their habitat (~15%) estimated as suitable for current and future niche availability. This region has been historically considered as a climate

refugium(Sun et al. 2017), particularly during the Pleistocene, and has supported the survival of various bird and mammal species during past environmental shifts (Chen et al. 2022; Chen et al. 2023), and hence can be a crucial future climate refugium for Tibetan Partridges. Developing and rehabilitating movement corridors to facilitate gene flow between populations, could aid in enhancing the adaptability of Tibetan partridges for short and long-term environmental changes.

Climate and biogeographic barriers shape evolutionary trajectories and population vulnerability in high-altitude species: The role of biogeographic barriers and climate in shaping species distributions, population divergence, and adaptation is a central question in ecology and evolutionary biology. While biogeographic influences are generally predictable, the interaction between climate and biogeography remains complex, particularly in the context of short and long-term environmental changes (De Kort et al. 2021). As global temperatures rise, precipitation patterns shift, and ecosystems transform, species must either adapt or face population decline and extinction. Examining divergence patterns and the mechanisms driving species' responses helps us understand the interaction between climate and biogeography and whether species exhibit similar or contrasting adaptations across their range. Gaining this knowledge not only enhances our understanding of the mechanistic basis of species adaptation but also aids in identifying vulnerable populations, predicting their future changes, and developing effective conservation strategies.

This knowledge is particularly crucial for species inhabiting high-altitude environments, where complex geography isolates local populations and creates contrasting environmental conditions within relatively small landscapes (Sánchez-Montes et al. 2018). However, the logistical challenges of collecting samples in these regions often result in sparse sampling across environmental and geographic gradients, limiting our ability to draw clear and comprehensive conclusions. In this study, we successfully examined multiple local populations of a high-altitude endemic species across broad geographical and environmental gradients throughout its distribution range. This comprehensive sampling allowed us to examine the role of biogeographic features, such as mountains and valleys, and climate in shaping its population distribution patterns and mechanisms of local adaptation. By integrating high-throughput genomic data with landscape and ecological information, we have revealed contrasting climatic

adaptations among populations across the species distribution range. Notably, we identify populations in drier regions as particularly vulnerable due to low genetic diversity, high genomic offsets, and reduced niche suitability under future climate change projections.

Our study provides valuable insights into the role of biogeography and climate shaping local adaptation of Tibetan Partridge populations across the Sino-Himalayan region, though these findings come with caveats. First, both predictive methods employed (genomic offset and niche modeling) have limitations (Costa et al. 2010; Rellstab et al. 2021). Genomic offset, as a relatively new concept, still requires more experimental validation (Rellstab et al. 2021). Moreover, the data supporting our predictions rely on genomic and environmental metrics without comprehensive information on actual population sizes. Additionally, our niche modeling was constrained by species distribution data, especially in the western range, which may affect the accuracy of ecological projections. While climate data served as a basis for niche predictions, other factors such as habitat connectivity and biotic interactions like predation and competition are likely also influential in shaping the estimated niche of Tibetan Partridge (Wisz et al. 2013). Despite these constraints, this study contributes valuable insights into historical events, current local adaptations, and future vulnerabilities of Tibetan Partridges in the context of short and long-term environmental changes.

In summary, species inhabiting diverse environmental and climatic gradient like those in the Sino-Himalayan region, characterized by significant climatic fluctuations, face rapid environmental changes that challenge their survival. Populations with low genetic diversity, limited suitable habitat, high genomic offset, and poor habitat connectivity are particularly at risk **(Fig. 5).** To address these challenges, generating robust data on population history, genetic variation associated with local adaptation, and identification of vulnerable habitats and populations are critical for species conservation. This study highlights the value of integrating morphological, ecological, and evolutionary perspectives to uncover comprehensive insights into species' historical dynamics, status, and future trajectories. Such an integrative approach is essential for designing and implementing effective conservation strategies that ensure the survival of species in the face of rapid environmental change.

Materials and Methods

Sample collection and genome re-sequencing: Blood samples were collected from 96 individuals of Tibetan Partridge across 28 different locations within the Qinghai-Tibetan Plateau (QTP) of the Sino-Himalayan landscape **(Fig. 1a)**. Eight of these populations are located to the west of the Yarlung Zangbo river and associated mountain ranges, while 20 are from the north-eastern regions, ensuring uniform sampling coverage across the distribution range of Tibetan Partridges.

Genomic DNA was extracted from samples using Qiagen's DNeasy Blood and Tissue kit (Qiagen, Valencia, CA, USA). Whole-genome re-sequencing was performed for each individual using the Illumina NovaSeq 6000 platform, and the raw sequencing reads were mapped against the previously published genome of Tibetan Partridge (Palacios et al. 2023) using BWA v0.7.17 with default settings (Li and Durbin 2009). Quality control of the mapped reads was conducted using PICARD (http://picard.sourceforge.net/) to remove PCR duplicates, followed by the Genome Analysis Toolkit (GATK) v.4.2.0.0(McKenna et al. 2010) and GATK best practices recommendations (Van der Auwera et al. 2013) to perform base quality recalibrations, insertion/deletion (INDEL) realignment, Single Nucleotide Polymorphism (SNP) discovery, and genotyping across all 96 samples. The variant filtering was done using a pipeline previously developed in the lab (Lamichhaney et al. 2015), applying the following filtering parameters: Fisher strand bias > 15, mapping quality < 50, mapping quality rank sum < -0.1, read position rank sum < -3, base quality rank sum < -5, depth > 4000 and < 500, quality by depth < 5, SNP quality > 100, and genotype quality > 10. Variants genotyped across all 96 samples were retained, and the final VCF file was generated using VCFTools v.0.1.13 (Danecek et al. 2011) for downstream analyses.

Morphological data collection: We measured morphological traits, including body length, tail length, and wing length using a flexible ruler. Beak length, head length, beak width, tarsus length, and middle toe claw length were measured with a vernier caliper, and body weight was recorded using an electronic scale. To account for body size variations, we adjusted the morphological data for body weight. These adjusted trait values were then used to assess

511 differences along the landscape through boxplots, Analysis of Variance (ANOVA), and principal
512 component analysis (PCA).

513 **Population genomics analysis:** We used a filtered set of 5,068,604 high-quality SNPs to assess
514 genetic diversity by computing population genetics parameters such as heterozygosity, and inter-
515 population genetic diversity (F_{ST}) using VCFtools v.0.1.13 (Danecek et al. 2011). To identify
516 phylogenetic relationships between samples we generated a maximum-likelihood phylogeny
517 using 93,160 SNPs in FastTree v.0.2.1 with recommended default parameters for nucleotide
518 alignments(Price et al. 2010). We further used SNAPP(Bryant et al. 2012) to estimate divergence
519 time between seven phylogenetic groups (two outgroups: Daurian partridge and Grey Partridge,
520 and individuals from six populations of Tibetan partridge across four different landscapes **(Fig.**
521 **1a)**, i. Western ii. Yarlung Zangbo high elevation iii. Yarlung Zangbo, 2900m elevation iv.
522 Hengduanshan (Nanjiang valley) v. Hengduanshan (Sichuan) vi. Qilianshan, based on
523 phylogenetic tree structure and known geographical barriers. We used Yarlung Zangbo's 2900 m
524 population and two populations from Hengduanshan (Sichuan and Nanjiang) to build a
525 divergence timeline of different populations. We used the divergence time of genus *Perdix* genus
526 diverged at 4.37 MYA (http://www.timetree.org/) to constraint with 0 offsets and a standard
527 deviation of 0.005 million years. We ran BEAST v.2.6.3 (Bouckaert et al. 2019) for 5 million
528 generations, with sampling conducted every 250 generations; the initial 10% was discarded as
529 burn-in. We ran Tracer 1.7.2 (Rambaut et al. 2018) to ensure convergence of all parameters (ESS
530 > 200) and TreeAnnotator 2.6.4 (Drummond and Rambaut 2007) to generate the maximum clade
531 credibility tree.
532
533 We also estimated ancestry using a maximum-likelihood approach in Admixture
534 v.1.3.0(Alexander et al. 2009) and plotted the admixture patterns across the landscapes using
535 Mapmixture v.0.1.0(Jenkins 2024) in R. The optimal number of genetic ancestries was selected
536 using a cross-validation procedure with the K-means method implemented in Admixture. To
537 examine the pattern of isolation by distance (IBD) and isolation by environment (IBE), we
538 performed the multiple regression for distance matrices (MRM) with 999 permutationst using
539 genetic distance (F_{ST}), geographic distance (km), and Euclidean distance of selected
540 environmental variables (BIO2, BIO8, and BIO9, BIO12, BIO15, see GEA below for details)
541 using the ecodist package(Lichstein 2007) in R.

542 **Genotype Environment Association (GEA) analysis:** We employed a combination of two
543 independent approaches to identify genomic regions associated with bioclimatic variables. First,
544 we utilized the Latent Factor Mixed Model (LFMM), a univariate analysis method that detects
545 associations between allele frequencies and climatic variables (Frichot et al. 2013). To account
546 for population structure in the dataset, we incorporated four latent factors identified by admixture
547 analysis. We conducted five independent Markov Chain Monte Carlo (MCMC) runs, with a
548 burn-in period of 5,000 iterations followed by 10,000 iterations. The results from these five runs
549 were averaged and adjusted for multiple testing, applying a false discovery rate (FDR) correction
550 of 1% as the significance threshold to identify candidate SNPs. To further validate and ensure the
551 accurate identification of candidate SNPs, we calculated the Fixation index (F_{ST}) between two
552 groups (five individuals each exposed to high and low values for each bioclimatic variable) using
553 the candidate SNPs generated by LFMM alongside a comparable number of randomly selected
554 SNPs across the genome.
555
556 The environmental variables for the multivariate analysis were carefully chosen based on
557 correlation analysis and their importance ranking derived from gradient forest analysis,
558 implemented using the R package "gradientForest"(Ellis et al. 2012). This approach ensured the
559 inclusion of relevant variables while minimizing redundancy in the analysis. Due to
560 computational limitations, we only used ~500,000 SNPs from the longest scaffold (Scaffold 738)
561 for this analysis. The selected predictors included three temperature-related variables: BIO2
562 (Mean Diurnal Range, calculated as the mean of monthly maximum temperature minus
563 minimum temperature), BIO8 (Mean Temperature of Wettest Quarter), and BIO9 (Mean
564 Temperature of Driest Quarter), as well as two precipitation-related variables: BIO12 (Annual
565 Precipitation) and BIO15 (Precipitation Seasonality, measured as the Coefficient of Variation)
566 **(Supplementary Fig. 3)**.
567
568 Next, we employed Redundancy Analysis (RDA), a multivariate approach, to examine the
569 relationship between multiple environmental variables and SNPs using the vegan package in
570 R(Capblancq and Forester 2021; Oksanen et al. 2024). Genetic variations associated with the
571 environment were considered significant if they had loadings in the tails of the distribution,

572 specifically within a standard deviation limit of 3.5 along the first three RDA axes, as
573 recommended in(Forester et al. 2018).
574
575 To perform functional analysis of the candidate genomic regions, we annotated the filtered VCF
576 file using the published genome of Tibetan Partridge(Palacios et al. 2023) using SnpEFF
577 (Cingolani et al. 2012). We then conducted Gene Ontology (GO) term analysis to identify
578 enriched GO terms among the candidate SNPs, comparing them against the background
579 annotated gene universe in the reference genome in R. First, we annotated the Tibetan partridge
580 transcriptome previously published(Palacios et al. 2023) using eggNOG-mapper (Cantalapiedra
581 et al. 2021) with the default parameters for characterizing Gene Ontology (GO) terms. We then
582 constructed an organism database (OrgDB) library for Tibetan partridge using the
583 makeOrgPackage function of AnnotationForge package (Carlson and Pagès 2024) in R. Gene Ids
584 of the climate-associated candidate SNPs were extracted and GO enrichment analysis was done
585 using the enrichGO and enricher functions from tclusterProfiler (Wu et al. 2021) package in R.
586 We considered GO terms with adjusted p-value and q-value < 0.05 as statistically significant
587 enrichment.
588
589 **Genomic offset prediction**: We used a machine learning-based non-parametric modeling
590 approach to predict allelic turnover under future climatic conditions, using the R package
591 gradientForest(Ellis et al. 2012). This method calculates genetic offset as the Euclidean distance
592 between genomic compositions in the current and predicted future climatic scenarios. To carry
593 out this analysis, we downloaded three general circulation models (GCMs)— FIO-ESM-2, IPSL-
594 CM6A-LR, and UKESM1-0-LL, from the Worldclim database (http://www.worldclim.org) (Fick
595 and Hijmans 2017). These models correspond to two carbon emission scenarios based on shared
596 socioeconomic pathways (SSPs): SSP 4.5 (moderate) and SSP 8.5 (harsh), for two time periods:
597 2061-2080 and 2081-2100, all at a resolution of 30 seconds. For each given GCM, time period,
598 and SSPs, we built GF models (12 models) and estimated the genetic offset for the same five
599 bioclimatic variables previously used in Gene-Environment Analysis. We averaged the
600 predictions for each SSPs across the two time periods, yielding four overall predictions (SSPs
601 4.5-year 2070, SSPs 8.5 year 2070, SSPs 4.5 year 2090, and SSPs 8.5 year 2090). We used the

602 Wilcoxon rank test to quantify the pairwise statistical difference of genomic offset between four
603 landscapes.
604

605 **Niche modeling:** To assess the current climatic niche and predict future suitability for the
606 Tibetan Partridge, we utilized occurrence data of Tibetan Partridge collected from field sampling
607 and the GBIF database (GBIF 2023). After filtering occurrences at a 1-km resolution, we
608 retained a total of 230 data points, with 96 occurrences from the eastern range and 134 from the
609 western range. We modeled these two ranges separately to identify bioclimatic variables that
610 serve as significant predictors of niche suitability. We used the same bioclimatic data
611 downloaded for genomic offset predictions used above. We further employed the USDM
612 (version 2.1) package (Naimi et al. 2014) in R to assess the variance inflation factor (VIF) and
613 identified multicollinearity among predictor variables, removing any variables with a VIF greater
614 than 2.5. Additionally, we evaluated the variable importance using the Biomod2 package
615 (Thuiller et al. 2016), retaining only those with higher variable importance.
616

617 We further utilized an ensemble modeling approach within the Biomod2 package (Thuiller et al.
618 2016) in R to assess species distribution under both current and future climatic scenarios. For
619 modeling, we randomly sampled 1,000 background points for both the western and north-eastern
620 landscapes. We applied three iterations of the cross-validation procedure, randomly dividing
621 occurrence records into two subsets: 70% of the data for model calibration and the remaining
622 30% for testing. Model evaluation was based on the Receiver Operating Characteristic (ROC), a
623 threshold-independent indicator of model performance (Hanley and McNeil 1982), and the True
624 Skill Statistic (TSS), which is calculated as the sum of sensitivity and specificity minus one
625 (Allouche et al. 2006). The predictions from various modeling algorithms were summarized
626 using a weighted mean approach (Marmion et al. 2009), excluding models with a TSS of 0.60 or
627 lower in the final model construction.
628

629 **Landscape resistance surface analysis:** We employed a simplistic approach to map the
630 resistance surface across the Tibetan Partridge's distribution range, drawing from the
631 methodology of a previous study (Chen et al. 2022). To calculate the resistance surface, we first
632 computed the average values of key landscape features (elevation, standard deviation of

elevation, and slope) using the current distribution of Tibetan Partridges as a reference. For each grid in the study area, we calculated the absolute difference between the value of each landscape feature and the average value of that feature based on the current distribution. A smaller difference indicated lower resistance, while a larger difference suggested greater resistance to movement. Next, we incorporated habitat suitability information into the resistance surface by subtracting the value of each grid from the highest suitability value, where a lower resultant value indicated lower resistance. To make the resistance surface easier to visualize and interpret, we rescaled the average of these continuous landscape values and habitat suitability to a scale from 1 (lowest resistance) to 10 (highest resistance) (Chen et al. 2022).

Acknowledgements: The fieldwork and genome sequencing were supported by the Central Forestry and Grassland Ecological Protection and Restoration Fund in Qinghai Province, the National Survey on Terrestrial Wildlife Resources in China, and The Abundance, Distribution, and Habitat of Leopards and Their Main Preys in Eastern Xizang (LC-3-04) to NW. PG was supported by a graduate assistantship from Kent State University. We express our gratitude to the personnel at the National Forestry and Grassland Administration of China, and the Forestry and Grassland Administration of Qinghai, Tibetan, and Sichuan provinces, China, for their unwavering support throughout the project. Special thanks to Hongtao Mao, Honglei Li, Qinze Zhang, Jiahu Jiang, Yichuan Meng, and Rong Liu for their contribution to the fieldwork associated with this study. We are thankful to Dr. Kristen Ruegg and Dr. Joan Ferrer Obiol for their insightful comments on the first draft of the manuscript. We also thank Neeraja V, Nick Addey, and Macauley Library at Cornell Lab of Ornithology for permitting us to use their photographs in this paper.

References

Alexander DH, Novembre J, Lange K. 2009. Fast model-based estimation of ancestry in unrelated individuals. *Genome Res.* 19:1655–1664.

Allouche O, Tsoar A, Kadmon R. 2006. Assessing the accuracy of species distribution models: prevalence, kappa and the true skill statistic (TSS). *J. Appl. Ecol.* 43:1223–1232.

Bay RA, Harrigan RJ, Underwood VL, Gibbs HL, Smith TB, Ruegg K. 2018. Genomic signals of selection predict climate-driven population declines in a migratory bird. *Science* 359:83–86.

Bouckaert R, Vaughan TG, Barido-Sottani J, Duchêne S, Fourment M, Gavryushkina A, Heled J, Jones G, Kühnert D, Maio ND, et al. 2019. BEAST 2.5: An advanced software platform for Bayesian evolutionary analysis. *PLOS Comput. Biol.* 15:e1006650.

Brown JH. 1984. On the Relationship between Abundance and Distribution of Species. *Am. Nat.* 124:255–279.

Bryant D, Bouckaert R, Felsenstein J, Rosenberg NA, RoyChoudhury A. 2012. Inferring Species Trees Directly from Biallelic Genetic Markers: Bypassing Gene Trees in a Full Coalescent Analysis. *Mol. Biol. Evol.* 29:1917–1932.

Busetto L, Ranghetti L. 2016. *MODIStsp*: An R package for automatic preprocessing of MODIS Land Products time series. *Comput. Geosci.* 97:40–48.

Cantalapiedra CP, Hernández-Plaza A, Letunic I, Bork P, Huerta-Cepas J. 2021. eggNOG-mapper v2: Functional Annotation, Orthology Assignments, and Domain Prediction at the Metagenomic Scale. *Mol. Biol. Evol.* 38:5825–5829.

Capblancq T, Forester BR. 2021. Redundancy analysis: A Swiss Army Knife for landscape genomics. *Methods Ecol. Evol.* 12:2298–2309.

Carlson M, Pagès H. 2024. AnnotationForge: Tools for building SQLite-based annotation data packages. Available from: http://bioconductor.org/packages/AnnotationForge/

Chen Y, Ge D, Ericson PGP, Song G, Wen Z, Luo X, Yang Q, Lei F, Qu Y. 2023. Alpine burrow-sharing mammals and birds show similar population-level climate change risks. *Nat. Clim. Change* 13:990–996.

Chen Y, Jiang Z, Fan P, Ericson PGP, Song G, Luo X, Lei F, Qu Y. 2022. The combination of genomic offset and niche modelling provides insights into climate change-driven vulnerability. *Nat. Commun.* 13:4821.

Cingolani P, Platts A, Wang LL, Coon M, Nguyen T, Wang L, Land SJ, Lu X, Ruden DM. 2012. A program for annotating and predicting the effects of single nucleotide polymorphisms, SnpEff. *Fly (Austin)* 6:80–92.

Colwell RK, Brehm G, Cardelús CL, Gilman AC, Longino JT. 2008. Global Warming, Elevational Range Shifts, and Lowland Biotic Attrition in the Wet Tropics. *Science* 322:258–261.

Costa GC, Nogueira C, Machado RB, Colli GR. 2010. Sampling bias and the use of ecological niche modeling in conservation planning: a field evaluation in a biodiversity hotspot. *Biodivers. Conserv.* 19:883–899.

Cui H, Wang J, Yu B, Hu Z, Yao P, Harbor JM. 2018. Marine Isotope Stage 3 paleotemperature inferred from reconstructing the Die Shan ice cap, northeastern Tibetan Plateau. *Quat. Res.* 89:494–504.

Danecek P, Auton A, Abecasis G, Albers CA, Banks E, DePristo MA, Handsaker RE, Lunter G, Marth GT, Sherry ST, et al. 2011. The variant call format and VCFtools. *Bioinformatics* 27:2156–2158.

De Kort H, Prunier JG, Ducatez S, Honnay O, Baguette M, Stevens VM, Blanchet S. 2021. Life history, climate and biogeography interactively affect worldwide genetic diversity of plant and animal populations. *Nat. Commun.* 12:516.

Deng T, Ding L. 2015. Paleoaltimetry reconstructions of the Tibetan Plateau: progress and contradictions. *Natl. Sci. Rev.* 2:417–437.

Descombes P, Leprieur F, Albouy C, Heine C, Pellissier L. 2017. Spatial imprints of plate tectonics on extant richness of terrestrial vertebrates. *J. Biogeogr.* 44:1185–1197.

Drummond AJ, Rambaut A. 2007. BEAST: Bayesian evolutionary analysis by sampling trees. *BMC Evol. Biol.* 7:214.

Du FK, Wang T, Wang Y, Ueno S, de Lafontaine G. 2020. Contrasted patterns of local adaptation to climate change across the range of an evergreen oak, Quercus aquifolioides. *Evol. Appl.* 13:2377–2391.

Ellis N, Smith SJ, Pitcher CR. 2012. Gradient forests: calculating importance gradients on physical predictors. *Ecology* 93:156–168.

Favre A, Päckert M, Pauls SU, Jähnig SC, Uhl D, Michalak I, Muellner-Riehl AN. 2015. The role of the uplift of the Qinghai-Tibetan Plateau for the evolution of Tibetan biotas. *Biol. Rev.* 90:236–253.

Fick SE, Hijmans RJ. 2017. WorldClim 2: new 1-km spatial resolution climate surfaces for global land areas. *Int. J. Climatol.* 37:4302–4315.

Forester BR, Lasky JR, Wagner HH, Urban DL. 2018. Comparing methods for detecting multilocus adaptation with multivariate genotype–environment associations. *Mol. Ecol.* 27:2215–2233.

Freeman BG, Scholer MN, Ruiz-Gutierrez V, Fitzpatrick JW. 2018. Climate change causes upslope shifts and mountaintop extirpations in a tropical bird community. *Proc. Natl. Acad. Sci.* 115:11982–11987.

Frichot E, Schoville SD, Bouchard G, François O. 2013. Testing for Associations between Loci and Environmental Gradients Using Latent Factor Mixed Models. *Mol. Biol. Evol.* 30:1687–1699.

Fuller A, Mitchell D, Maloney SK, Hetem RS, Fonsêca VFC, Meyer LCR, van de Ven TMFN, Snelling EP. 2021. How dryland mammals will respond to climate change: the effects of body size, heat load and a lack of food and water. *J. Exp. Biol.* 224:jeb238113.

GBIF. 2023. GBIF Occurrence Download. Available from: GBIF.org

Hanley JA, McNeil BJ. 1982. The meaning and use of the area under a receiver operating characteristic (ROC) curve. *Radiology* 143:29–36.

Hu A, Wang Jianjun, Sun H, Niu B, Si G, Wang Jian, Yeh C-F, Zhu X, Lu X, Zhou J, et al. 2020. Mountain biodiversity and ecosystem functions: interplay between geology and contemporary environments. *ISME J.* 14:931–944.

Jenkins TL. 2024. mapmixture: An R package and web app for spatial visualisation of admixture and population structure. *Mol. Ecol. Resour.* 24:e13943.

Jiao X, Wu L, Zhang D, Wang H, Dong F, Yang L, Wang S, Amano HE, Zhang W, Jia C, et al. 2024. Landscape Heterogeneity Explains the Genetic Differentiation of a Forest Bird across the Sino-Himalayan Mountains. *Mol. Biol. Evol.* 41:msae027.

Kaushik R, Dige M, Rout P. 2016. Molecular Characterization and Expression Profiling of ENOX2 Gene in Response to Heat Stress in Goats. *Cell Dev. Biol.* 5:1–5.

Knight J. 2022. Scientists' warning of the impacts of climate change on mountains. *PeerJ* 10:e14253.

Kordonowy L, MacManes M. 2017. Characterizing the reproductive transcriptomic correlates of acute dehydration in males in the desert-adapted rodent, Peromyscus eremicus. *BMC Genomics* 18:473.

Laguë SL. 2017. High-altitude champions: birds that live and migrate at altitude. *J. Appl. Physiol.* 123:942–950.

Lamichhaney S, Berglund J, Almén MS, Maqbool K, Grabherr M, Martinez-Barrio A, Promerová M, Rubin C-J, Wang C, Zamani N. 2015. Evolution of Darwin's finches and their beaks revealed by genome sequencing. *Nature* 518:371–375.

Li H, Durbin R. 2009. Fast and accurate short read alignment with Burrows–Wheeler transform. *Bioinformatics* 25:1754–1760.

Lichstein JW. 2007. Multiple regression on distance matrices: a multivariate spatial analysis tool. *Plant Ecol.* 188:117–131.

Liu W, Zhao Y, Qi D, You J, Zhou Y, Song Z. 2018. The Tanggula Mountains enhance population divergence in Carex moorcroftii: a dominant sedge on the Qinghai-Tibetan Plateau. *Sci. Rep.* 8:2741.

Lu X, Ciren S. 2002. Habitat Selection and Flock Size of Tibetan Partridge Perdix hodgsoniae during Autumn-Winter. *J. Yamashina Inst. Ornithol.* 33:168–175.

Marmion M, Parviainen M, Luoto M, Heikkinen RK, Thuiller W. 2009. Evaluation of consensus methods in predictive species distribution modelling. *Divers. Distrib.* 15:59–69.

McGowan P, Madge S. 2010. Pheasants, Partridges & Grouse: Including buttonquails, sandgrouse and allies. A&C Black

McKenna A, Hanna M, Banks E, Sivachenko A, Cibulskis K, Kernytsky A, Garimella K, Altshuler D, Gabriel S, Daly M, et al. 2010. The Genome Analysis Toolkit: A MapReduce framework for analyzing next-generation DNA sequencing data. *Genome Res.* 20:1297–1303.

Naimi B, Hamm NAS, Groen TA, Skidmore AK, Toxopeus AG. 2014. Where is positional uncertainty a problem for species distribution modelling? *Ecography* 37:191–203.

Oksanen J, Simpson G, Blanchet FG, Kindt R, Legendre P, Minchin PR, O'Hara RB, Solymos P, Stevens MHH, Szoecs E, et al. 2024. vegan: Community Ecology Package. Available from: https://github.com/vegandevs/vegan

Owen LA, Finkel RC, Haizhou M, Spencer JQ, Derbyshire E, Barnard PL, Caffee MW. 2003. Timing and style of Late Quaternary glaciation in northeastern Tibet. *GSA Bull.* 115:1356–1364.

Palacios C, Wang P, Wang N, Brown MA, Capatosto L, Du J, Jiang J, Zhang Q, Dahal N, Lamichhaney S. 2023. Genomic Variation, Population History, and Long-Term Genetic Adaptation to High Altitudes in Tibetan Partridge (*Perdix hodgsoniae*).Yoder A, editor. *Mol. Biol. Evol.* 40:msad214.

Peters MK, Hemp A, Appelhans T, Becker JN, Behler C, Classen A, Detsch F, Ensslin A, Ferger SW, Frederiksen SB, et al. 2019. Climate–land-use interactions shape tropical mountain biodiversity and ecosystem functions. *Nature* 568:88–92.

Petkova D, Novembre J, Stephens M. 2016. Visualizing spatial population structure with estimated effective migration surfaces. *Nat. Genet.* 48:94–100.

Price MN, Dehal PS, Arkin AP. 2010. FastTree 2 – approximately maximum-likelihood trees for large alignments. *PLoS ONE* 5:e9490–e9490.

Rahbek C, Borregaard MK, Colwell RK, Dalsgaard B, Holt BG, Morueta-Holme N, Nogues-Bravo D, Whittaker RJ, Fjeldså J. 2019. Humboldt's enigma: What causes global patterns of mountain biodiversity? *Science* 365:1108–1113.

Rambaut A, Drummond AJ, Xie D, Baele G, Suchard MA. 2018. Posterior Summarization in Bayesian Phylogenetics Using Tracer 1.7. *Syst. Biol.* 67:901–904.

Rana SK, Rawal RS, Dangwal B, Bhatt ID, Price TD. 2021. 200 Years of Research on Himalayan Biodiversity: Trends, Gaps, and Policy Implications. *Front. Ecol. Evol.* [Internet] 8. Available from: https://www.frontiersin.org/articles/10.3389/fevo.2020.603422/full

Rellstab C, Dauphin B, Exposito-Alonso M. 2021. Prospects and limitations of genomic offset in conservation management. *Evol. Appl.* 14:1202–1212.

Rödder D, Schmitt T, Gros P, Ulrich W, Habel JC. 2021. Climate change drives mountain butterflies towards the summits. *Sci. Rep.* 11:14382.

Ruegg K, Bay RA, Anderson EC, Saracco JF, Harrigan RJ, Whitfield M, Paxton EH, Smith TB. 2018. Ecological genomics predicts climate vulnerability in an endangered southwestern songbird. *Ecol. Lett.* 21:1085–1096.

Sánchez-Montes G, Wang J, Ariño AH, Martínez-Solano Í. 2018. Mountains as barriers to gene flow in amphibians: Quantifying the differential effect of a major mountain ridge on the genetic structure of four sympatric species with different life history traits. *J. Biogeogr.* 45:318–331.

Sanlialp A, Schumacher D, Kiper L, Varma E, Riechert E, Ho TC, Hofmann C, Kmietczyk V, Zimmermann F, Dlugosz S, et al. 2020. Saraf-dependent activation of mTORC1 regulates cardiac growth. *J. Mol. Cell. Cardiol.* 141:30–42.

Stonehouse JC, Spurgin LG, Laine VN, Bosse M, The Great Tit HapMap Consortium, Groenen MAM, van Oers K, Sheldon BC, Visser ME, Slate J. 2024. The genomics of adaptation to climate in European great tit (Parus major) populations. *Evol. Lett.* 8:18–28.

Storz JF. 2021. High-Altitude Adaptation: Mechanistic Insights from Integrated Genomics and Physiology. *Mol. Biol. Evol.* 38:2677–2691.

Sun H, Zhang J, Deng T, Boufford DE. 2017. Origins and evolution of plant diversity in the Hengduan Mountains, China. *Plant Divers.* 39:161.

Thuiller W, Engler R, Breiner F. 2016. biomod2: Ensemble platform for species distribution modeling. R package version, 3(3), r539.

Turbek SP, Bossu C, Rayne C, Gruppi C, Kus BE, Whitfield M, Smith TB, Paxton EH, Bay RA, Ruegg KC. 2023. Historical DNA reveals climate adaptation in an endangered songbird. *Nat. Clim. Change* 13:735–741.

Van der Auwera GA, Carneiro MO, Hartl C, Poplin R, Del Angel G, Levy-Moonshine A, Jordan T, Shakir K, Roazen D, Thibault J, et al. 2013. From FastQ data to high confidence variant calls: the Genome Analysis Toolkit best practices pipeline. *Curr. Protoc. Bioinforma.* 43:11.10.1-33.

Verburg-van Kemenade BML, Cohen N, Chadzinska M. 2017. Neuroendocrine-immune system interactions: An evolutionary perspective preface. *Dev. Comp. Immunol.* 66:1–1.

Wang G, Yang Y, Zhang S, Lan H, Zheng X. 2022. The biological activity and signaling profile of EGF/EGFR were affected under heat stress conditions in IEC6 cells. *Gen. Comp. Endocrinol.* 325:114050.

Wang P, Scherler D, Liu-Zeng J, Mey J, Avouac J-P, Zhang Y, Shi D. 2014. Tectonic control of Yarlung Tsangpo Gorge revealed by a buried canyon in Southern Tibet. *Science* 346:978–981.

Wisz MS, Pottier J, Kissling WD, Pellissier L, Lenoir J, Damgaard CF, Dormann CF, Forchhammer MC, Grytnes J-A, Guisan A, et al. 2013. The role of biotic interactions in shaping distributions and realised assemblages of species: implications for species distribution modelling. *Biol. Rev.* 88:15–30.

Wu T, Hu E, Xu S, Chen M, Guo P, Dai Z, Feng T, Zhou L, Tang W, Zhan L, et al. 2021. clusterProfiler 4.0: A universal enrichment tool for interpreting omics data. *The Innovation* 2:100141.

Yamashiro S, Gokhin DS, Kimura S, Nowak RB, Fowler VM. 2012. Tropomodulins: pointed-end capping proteins that regulate actin filament architecture in diverse cell types. *Cytoskelet. Hoboken NJ* 69:337.

Yao H, Zhang Y, Wang Z, Liu G, Ran Q, Zhang Z, Guo K, Yang A, Wang N, Wang P. 2022. Inter-glacial isolation caused divergence of cold-adapted species: the case of the snow partridge. *Curr. Zool.* 68:489–498.

Figure legends

Figure 1: Distribution Range of the Tibetan Partridge and Environmental Variability Across the Sino-Himalayan Landscape (a) The map inset (top left) illustrates the Indian subcontinent for geographical reference. The main panel highlights the distribution range of the Tibetan Partridge, along with key mountains and geographical barriers. Sampling locations are represented by red circumpuncts, while black dots indicate known distribution points based on the eBird database. The high-elevation zone along the upper Yarlung Zangbo River is marked with a black triangle, and prominent mountain ranges include, the Himalayas (blue triangle), Gangdis Mountains (brown triangle with connecting brown line), and Nianqing Tanggula Mountains (white triangle), Qilian Mountains (green triangle). The Yellow River is depicted in yellow. The Tibetan Partridge populations west of the Nianqing Tanggula Mountains are noted for their distinctive black belly patch (bottom left image, © Neeraja V, ML621931282), contrasting with eastern populations that lack this feature (bottom right image, © Nick Addey, ML612172194) **(b)** Annual precipitation (mm) and **(c)** annual mean temperature (x10°C) maps highlight climatic variability across the distribution range.

Figure 2: Morphological and Genomic Evidence Reveal Geographic and Historical Isolation as Key Drivers of Genetic Structure in Tibetan Partridges (a) Beak length variation: adjusted beak length (mm) by body weight across landscapes shows an increasing

871 trend from the Western landscape to the Qilianshan region **(b)** Morphological PCA: Principal
872 Component Analysis (PCA) of nine morphological traits indicates two distinct clusters,
873 reflecting variation across Tibetan Partridge populations **(c)** Phylogenetic analysis: A maximum
874 likelihood phylogenetic tree constructed from 29,595,022 SNPs identifies the genetic structure of
875 Tibetan Partridge populations, strongly aligned with their respective landscapes. All major nodes
876 have local support > 0.9 based on the Shimodaira–Hasegawa test(Price et al. 2010) **(d)** Genetic
877 PCA: PCA based on genomic data reveals clustering patterns within populations, consistent with
878 the phylogenetic tree results, further validating the population structure **(e)** Admixture
879 proportions map: A distribution map displays the admixture proportions for individuals assigned
880 to each genetic cluster (K=4). Key geographical features are annotated, including the high-
881 elevation zone along the Yarlung Zangbo River (black triangles), the Nianqing Tanggula
882 Mountains (white triangles), and the Yellow River (yellow). This map was generated using the
883 Mapmixture v.0.1.061(Jenkins 2024) **(f)** EEMS Analysis: The Estimated Effective Migration
884 Surface (EEMS) illustrates migration rates with color contours: orange indicates low migration
885 rates, while blue signifies high migration rates. Color codes for each landscape are consistent
886 across all panels for clarity and comparison.

887 **Figure 3: Genetic Adaptations of Tibetan Partridge Populations to Local Climatic**
888 **Conditions (a)** Manhattan plot showing -$\log_{10}$(p) values from the Gene-Environment
889 Association (GEA) analysis for 5,068,604 SNPs with BIO9 (Mean Temperature of the Driest
890 Quarter) as the environmental variable. Candidate SNPs surpassing the red dashed line meet the
891 1% False Discovery Rate (FDR) correction threshold. The *SARAF* gene (*Store-operated calcium*
892 *entry-associated regulatory factor*) overlapping one of the top candidate SNP, is highlighted
893 within a circle **(b)** The allelic distribution of a candidate SNP (*Scaffold_631:373769*) within the
894 *SARAF* gene demonstrates a higher frequency of the C allele in populations inhabiting regions
895 with lower mean temperatures during the driest quarter (BIO9) **(c)** Manhattan plot
896 showing -log10(p) values for SNPs associated with BIO12 (Annual Precipitation). Candidate
897 SNPs surpassing the red dashed line meet the 1% False Discovery Rate (FDR) correction
898 threshold. The *TMOD1* gene (*Tropomodulin-1*), overlapping one of the top candidate SNP, is
899 highlighted within a circle **(d)** The allelic distribution of a candidate SNP (*Scaffold_720:849107*)
900 within the *TMOD1* gene reveals contrasting patterns: the T allele is nearly fixed in drier regions
901 (white), while the C allele dominates in wetter regions (blue) (e) Redundancy analysis showing

902 results of the first two axes **(e)** and first and third axis **(f)**; Each dot represents an individual bird,
903 color-coded by its population landscape (consistent with **Fig. 1**). Blue vectors represent the
904 direction and magnitude of correlation with environmental predictors represented by five
905 composite bioclimatic variables principal component. Populations from Hengduanshan and
906 Qilianshan landscapes are associated with precipitation-related variables (Annual Precipitation:
907 BIO12 and Precipitation Seasonality: BIO15), while populations from Western and Yarlung
908 Zangbo landscapes are associated with temperature-related variables (Mean Temperature of
909 Driest Quarter: BIO9, Mean Temperature of Wettest Quarter: BIO8, and Mean Diurnal Range:
910 BIO2).
911
912 **Figure 4: Climate change vulnerabilities in Tibetan Partridge populations revealed by**
913 **landscape-scale genomic offset and niche modeling across the Sino-Himalayan region.**
914 **(a)** Genomic offsets predicted by the gradientForest model under SSP245 scenarios for 2061–
915 2080 across the Tibetan Partridge distribution range **(b)** Genomic offsets are significantly higher
916 in the Western (n = 267,215 points), Yarlung Zangbo (n = 564,031 points), and Qilianshan (n =
917 1,030,066 points) landscapes, while the Hengduanshan landscape (n = 317,063 points) shows the
918 lowest genomic offset values ($p < 0.0001$ for all pairwise comparisons, two-tailed Wilcoxon
919 rank-sum test with FDR correction) **(c)** Current niche suitability model projected across the
920 Tibetan Partridge's distribution range **(d)** Proportions of suitable niche areas in each landscape
921 under current and future climatic scenarios (SSP4.5 for 2070/2090 and SSP8.5 for 2070/2090)
922 **(e)** Resistance surface map showing higher landscape connectivity (green) in the Hengduanshan
923 and Qilianshan landscapes in the northeast compared to reduced connectivity in the Yarlung
924 Zangbo and Western landscapes **(f)** Proportion of heterozygous sites in local Tibetan Partridge
925 populations, indicating reduced heterozygosity in the Western landscape.
926
927 **Figure 5:** Conceptual framework of using genomic, ecological, and landscape information to
928 understand climatic vulnerability. Past geological events shape the distribution of species such
929 that the formation of barriers and subsequent local adaptation promote population divergence.
930 These populations are exposed to varying levels of climatic vulnerability depending upon their
931 genetics, ecology, and landscape connectivity.

932 **Supplementary Figures legends**

933 **Supplementary Figure 1: Morphological trait variation among Tibetan Partridge**
934 **populations residing across different landscapes (a)** Body length, **(b)** Left paw length, **(c)**
935 Right paw length, **(d)** Tail length, **(e)** Left-wing length, **(f)** Right-wing length, **(g)** Left
936 tarsometatarsus length, and **(h)** Right tarsometatarsus length. P-values displayed are derived
937 from Analysis of Variance (ANOVA), with $p < 0.05$ denoting significant differences in trait
938 values across landscapes at the 95% confidence interval. Adjusted value for each trait calculated
939 by dividing raw measure by body weight.

940

941 **Supplementary Figure 2: Topographic and vegetational heterogeneity in the Sino-**
942 **Himalayan region (a)** 3-dimensional elevation map highlighting significant elevation variability
943 across the landscape, with high-elevation regions (in yellow) aligned with key topographic
944 features indicated in Fig. 1, contrasting with the plateau areas in the northeast (green), which
945 range from 4000m to 5000m. (map source: WorldviewR: https://jcallura.github.io/) **(b)** The
946 Normalized Difference Vegetation Index (NDVI) map shows vegetation density differences
947 across the distribution range. The northeast region exhibits higher vegetation cover, while
948 western areas have relatively sparse vegetation. (Data source: MODIS 16-day vegetation index, 1
949 km resolution, for June 1, 2020, processed using MODIStsp in R(Busetto and Ranghetti 2016).

950 **Supplementary Figure 3: Variation in sequencing coverage of individual samples across**
951 **landscape.** Gray dot refers to each individual sample's coverage**.**

952 **Supplementary Figure 4: Molecular dating and genetic divergence in Tibetan Partridge**
953 **populations (a)** Molecular dating analysis indicates recent divergence within Tibetan partridge
954 populations, with divergence times ranging from 0.33 to 0.05 million years ago (mya). The
955 north-eastern and western populations, separated by the Nianqing Tanggula mountains, diverged
956 around 0.33 mya. The population along the Nujiang River in the Hengduanshan landscape,
957 northeast of the Nianqing Tanggula mountains, diverged from the plateau population
958 approximately 0.10 mya. The Yarlung Zangbo and Western populations, separated by high-
959 elevation zones along the upper Yarlung Zangbo river, diverged around 0.05 mya; the most
960 recent divergence within Tibetan partridges is low elevation movement to 2900 m. Genetic

variation across landscapes can be poorly explained by (b) Isolation by Distance (IBD), though its effects are relatively weak(($\beta = 0.0000433$, $p = 0.125$). In contrast, (c) Isolation by Environment (IBE) has a stronger and more significant influence $\beta = 0.0771$, $p = 0.001$)

Supplementary Figure 5: Gradient forest analysis highlights precipitation-related variables (blue) as the strongest predictors of genetic variation in Tibetan Partridges
(a) Ranked importance of variables based on prediction accuracy and **(b)** R-squared weighted importance reveals the dominance of precipitation-related factors. Variables in grey were excluded from further modeling to prioritize climate-related predictors.

Supplementary Figure 6: Manhattan plot showing -$\log_{10}$(p) values from Gene Environment Association (GEA) analysis to identify association with bioclimatic variables (a) BIO2 (Mean Diurnal Range) **(b)** BIO8 (Mean Temperature of Wettest Quarter) and **(c)** BIO15 (Precipitation Seasonality). SNPs above the red dashed line denote candidate SNPs after a significance threshold of 1% False Discovery Rate (FDR) correction.

Supplementary Figure 7: Distribution of genetic differentiation (F_{ST}) for "climate-associated core" candidate SNPs vs. random SNPs, for **(a)** BIO2 (Mean Diurnal Range) **(b)** BIO8 (Mean Temperature of Wettest Quarter) **(c)** BIO9 (Mean Temperature of Driest Quarter) **(d)** BIO12 (Annual Precipitation) and **(e)** BIO15 (Precipitation Seasonality). F_{ST} calculations were based on ten individuals each from populations exposed to the highest and lowest values for each respective bioclimatic variable.

Supplementary Figure 8: Venn diagram illustrating the overlap of candidate SNPs identified by univariate (LFMM) and multivariate (RDA) analyses associated with bioclimatic variables; center: overlapping SNPs identified by both LFMM and RDA, suggesting robust associations with climatic adaptation, lower left: number of SNPs identified by LFMM analysis for individual bioclimatic variables, with precipitation-related variables shown in green and temperature-related variables in red in the right table.

Supplementary Figure 9: The gradientForest predicted genomic offsets (a) under *SSP 8.5* for the year 2070 ($p < 2e^{-16}$ for all pairwise comparisons, the two-tailed Wilcoxon rank-sum test and FDR correction for multiple comparisons) **(b)** under *SSP 4.5* for the year 2090 ($p < 2e^{-16}$ for all pairwise comparison, the two-tailed Wilcoxon rank-sum test and FDR correction for multiple

comparisons) and **(c)** under *SSP 8.5* for the year 2090 ($p < 2e^{-16}$ for all pairwise comparison, the two-tailed Wilcoxon rank-sum test and FDR correction for multiple comparisons). *SSP 8.5* is the worst climatic conditions and *SSP 4.5* is moderate climatic conditions. The distribution of predicted genomic offset across each landscape is shown in the right panel for each figure.

Data availability: All short-read whole-genome sequencing data have been submitted to the National Center for Biotechnology Information (NCBI) under BioProject Accession number PRJNA1198335.

Code availability: Scripts and workflow for all analyses done in this paper is available on the GitHub page https://github.com/Prashantevo/Tibetanpatridgeeeb.

Competing interests: The authors declare no competing interests.

Additional information

Supplementary Materials

Supplementary Resources 1 - 2

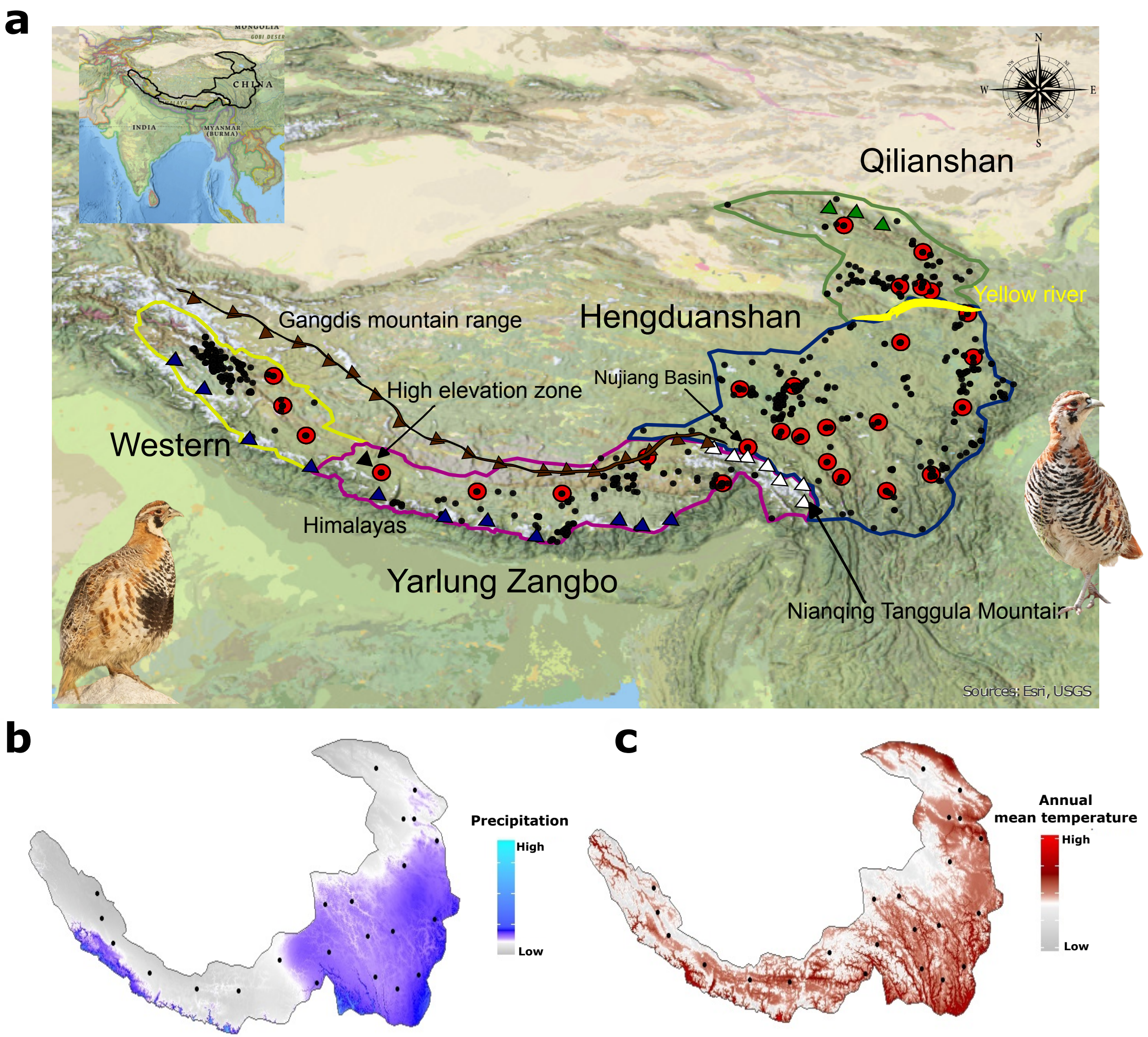

Figure 1: Distribution Range of the Tibetan Partridge and Environmental Variability Across the Sino-Himalayan Landscape (a) The map inset (top left) illustrates the Indian subcontinent for geographical reference. The main panel highlights the distribution range of the Tibetan Partridge, along with key mountains and geographical barriers. Sampling locations are represented by red circumpuncts, while black dots indicate known distribution points based on the eBird database. The high-elevation zone along the upper Yarlung Zangbo River is marked with a black triangle, and prominent mountain ranges include, Himalayas (blue triangle), Gangdis Mountains (brown triangle with connecting brown line), and Nianqing Tanggula Mountains (white triangle), Qilian Mountains (green triangle). The Yellow River is depicted in yellow. The Tibetan Partridge populations west of the Nianqing Tanggula Mountains are noted for their distinctive black belly patch (bottom left image, © Neeraja V, ML621931282), contrasting with eastern populations that lack this feature (bottom right image, © Nick Addey, ML612172194) **(b)** Annual precipitation (mm) and **(c)** annual mean temperature (°C) maps highlight climatic variability across the distribution range.

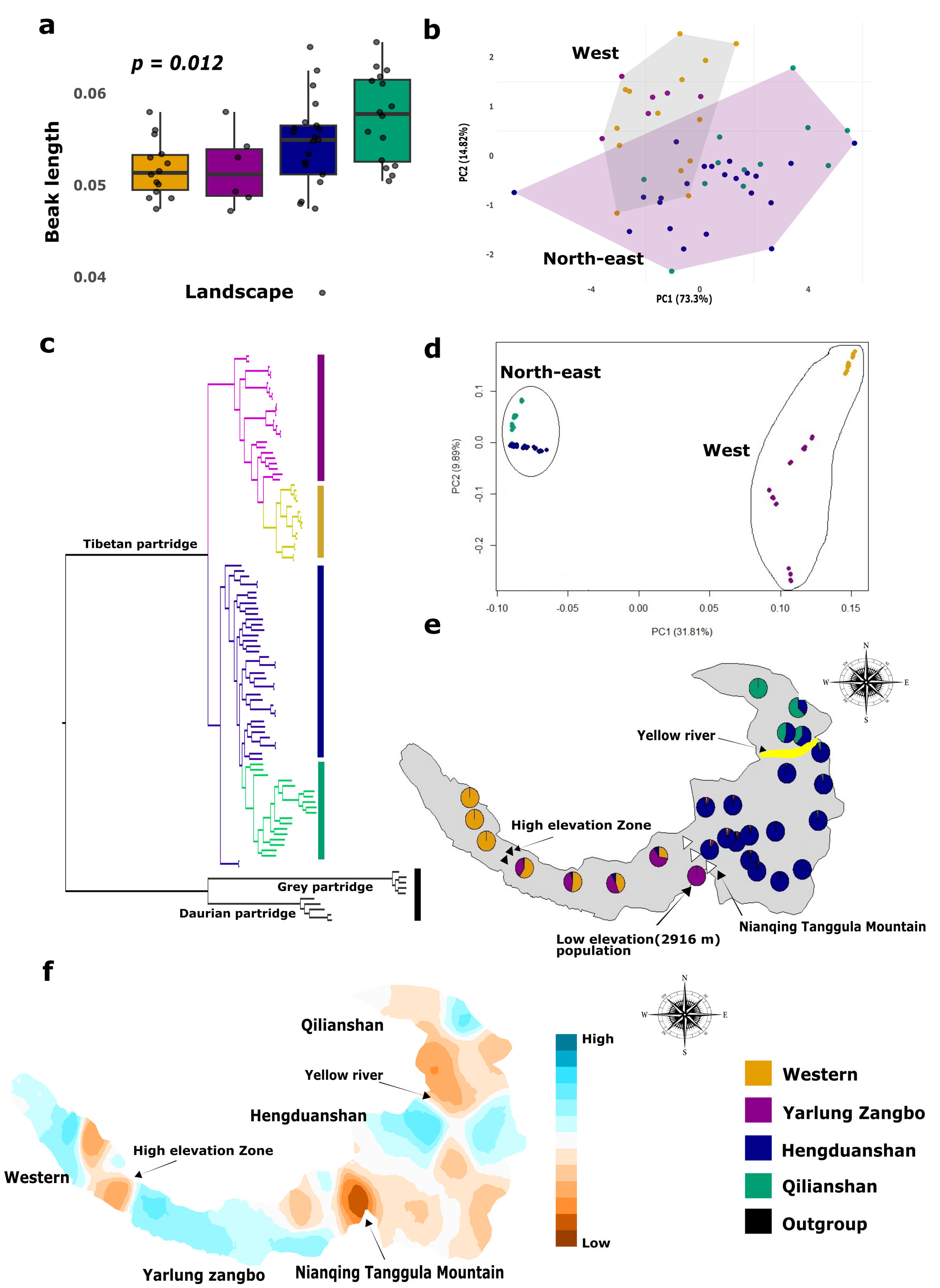

Figure 2: Morphological and Genomic Evidence Reveal Geographic and Historical Isolation as Key Drivers of Genetic Structure in Tibetan Partridges (a) Beak length variation: adjusted beak length (mm) by body weight across landscapes shows an increasing trend from the Western landscape to the Qilianshan region **(b)** Morphological PCA: Principal Component Analysis (PCA) of nine morphological traits indicates two distinct clusters, reflecting variation across Tibetan Partridge populations **(c)** Phylogenetic analysis: A maximum likelihood phylogenetic tree constructed from 29,595,022 SNPs identifies the genetic structure of Tibetan Partridge populations, strongly aligned with their respective landscapes. All major nodes have local support > 0.9 based on the Shimodaira–Hasegawa test[55] **(d)** Genetic PCA: PCA based on genomic data reveals clustering patterns within populations, consistent with the phylogenetic tree results, further validating the population structure **(e)** Admixture proportions map: A distribution map displays the admixture proportions for individuals assigned to each genetic cluster (K=4). Key geographical features are annotated, including the high-elevation zone along the Yarlung Zangbo River (black triangles), Nianqing Tanggula Mountains (white triangles), and the Yellow River (yellow). This map was generated using the Mapmixture v.0.1.061[61] **(f)** EEMS Analysis: The Estimated Effective Migration Surface (EEMS) illustrates migration rates with color contours: orange indicates low migration rates, while blue signifies high migration rates. Color codes for each landscape are consistent across all panels for clarity and comparison.

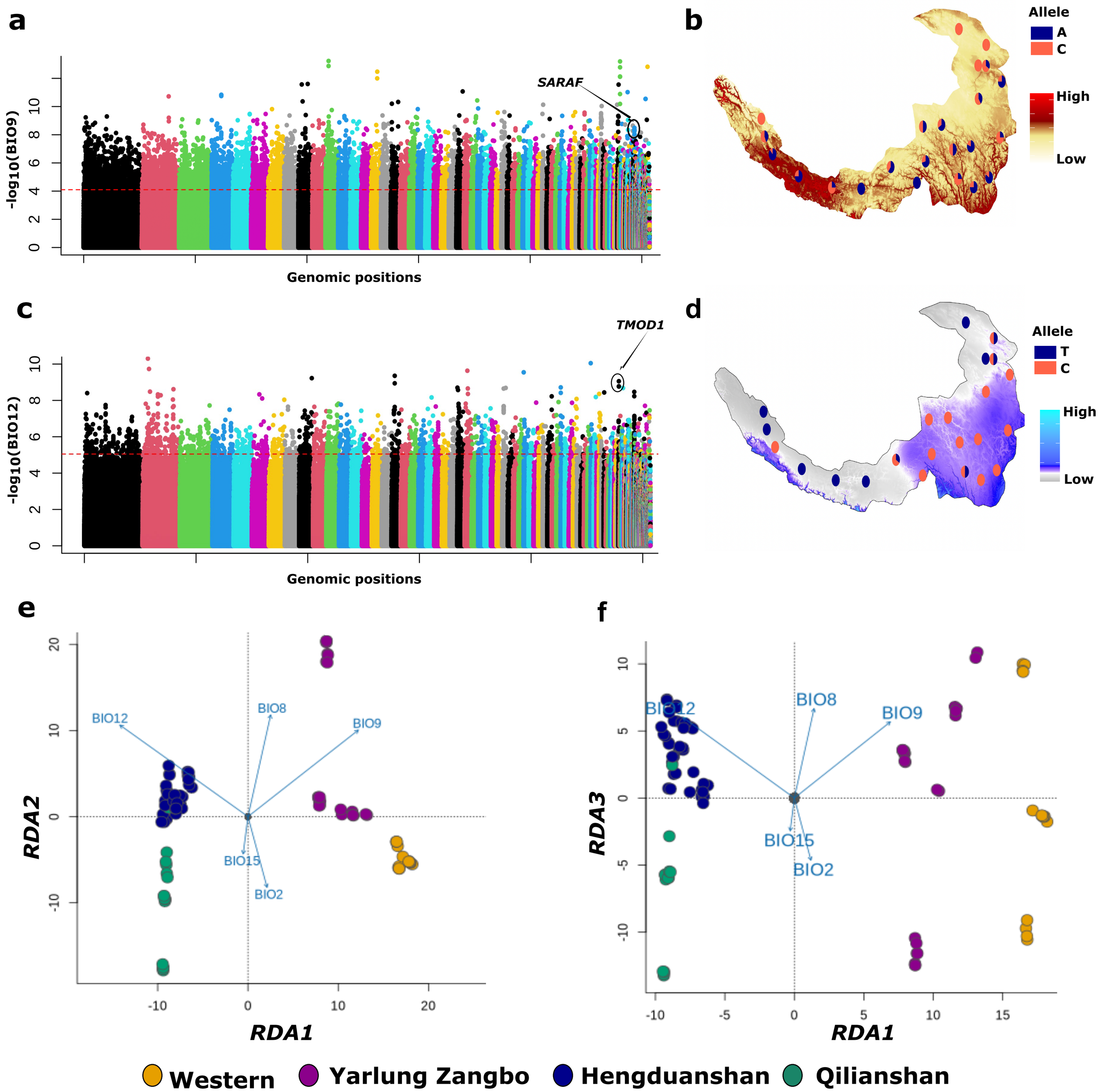

Figure 3: Genetic Adaptations of Tibetan Partridge Populations to Local Climatic Conditions
(a) Manhattan plot showing -$\log_{10}$(p) values from the Gene-Environment Association (GEA) analysis for 5,068,604 SNPs with BIO9 (Mean Temperature of the Driest Quarter) as the environmental variable. Candidate SNPs surpassing the red dashed line meet the 1% False Discovery Rate (FDR) correction threshold. The *SARAF* gene *(Store-operated calcium entry-associated regulatory factor)* overlapping one of the top candidate SNP, is highlighted within a circle **(b)** The allelic distribution of a candidate SNP (Scaffold_631:373769) within the *SARAF* gene demonstrates a higher frequency of the C allele in populations inhabiting regions with lower mean temperatures during the driest quarter (BIO9) **(c)** Manhattan plot showing -$\log_{10}$(p) values for SNPs associated with BIO12 (Annual Precipitation). Candidate SNPs surpassing the red dashed line meet the 1% False Discovery Rate (FDR) correction threshold. The *TMOD1* gene *(Tropomodulin-1)*, overlapping one of the top candidate SNP, is highlighted within a circle **(d)** The allelic distribution of a candidate SNP (Scaffold_720:849107) within the *TMOD1* gene reveals contrasting patterns: the T allele is nearly fixed in drier regions (white), while the C allele dominates in wetter regions (blue). Redundancy analysis showing results of the first two axes **(e)** and first and third axis **(f)**; Each dot represents an individual bird, color-coded by its population landscape (consistent with **Fig. 1**). Blue vectors represent the direction and magnitude of correlation with environmental predictors represented by five composite bioclimatic variables principle component. Populations from Hengduanshan and Qilianshan landscapes are associated with precipitation-related variables (Annual Precipitation: BIO12 and Precipitation Seasonality: BIO15), while populations from Western and Yarlung Zangbo landscapes are associated with temperature-related variables (Mean Temperature of Driest Quarter: BIO9, Mean Temperature of Wettest Quarter: BIO8, and Mean Diurnal Range: BIO2).

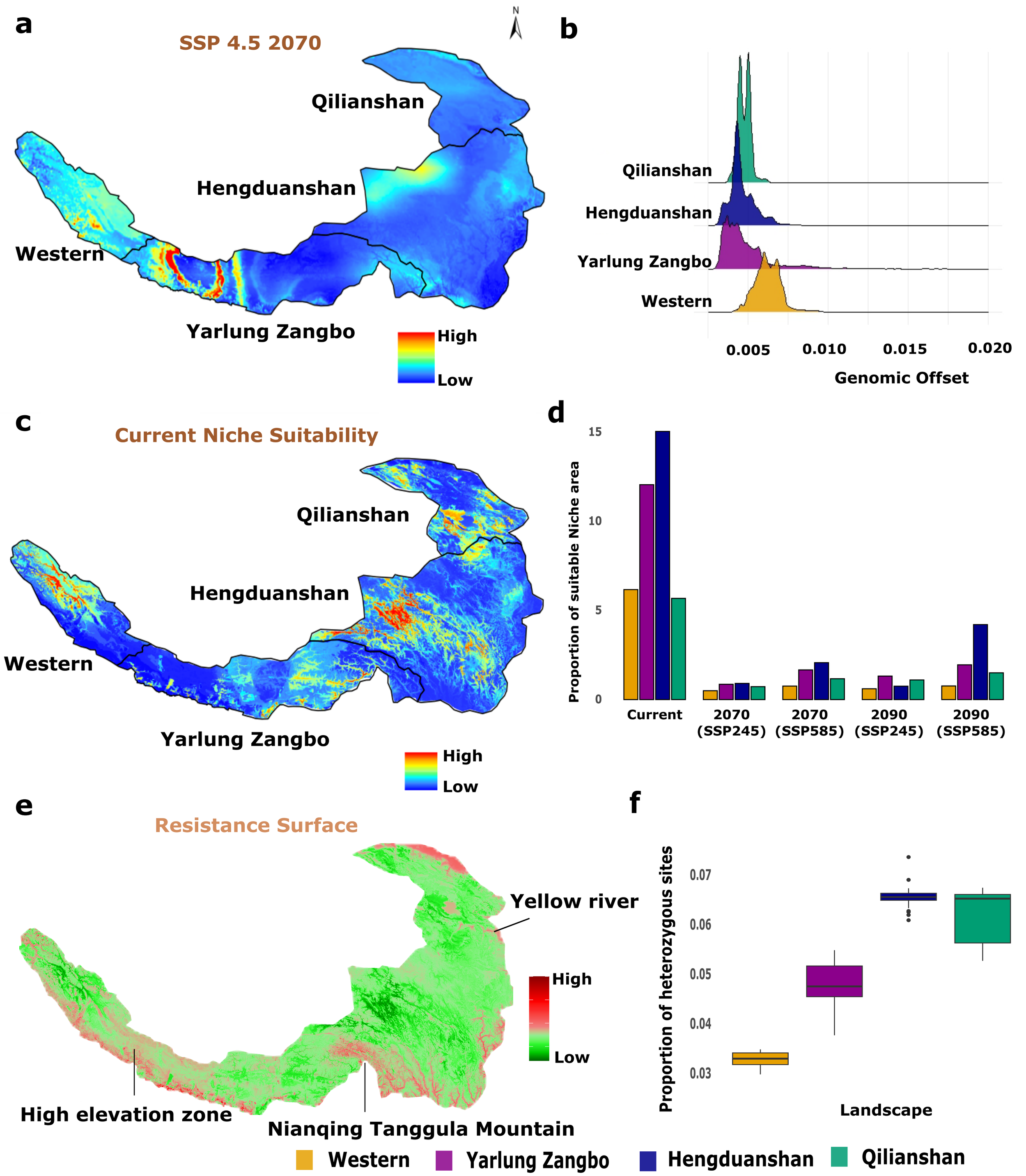

Figure 4: Climate change vulnerabilities in Tibetan Partridge populations revealed by landscape-scale genomic offset and niche modeling across the Sino-Himalayan region (a) Genomic offsets predicted by the gradientForest model under *SSP245* scenarios for 2061–2080 across the Tibetan Partridge distribution range **(b)** Genomic offsets are significantly higher in the Western (n = 267,215 points), Yarlung Zangbo (n = 564,031 points), and Qilianshan (n = 1,030,066 points) landscapes, while the Hengduanshan landscape (n = 317,063 points) shows the lowest genomic offset values (*p < 0.0001* for all pairwise comparisons, two-tailed Wilcoxon rank-sum test with FDR correction) **(c)** Current niche suitability model projected across the Tibetan Partridge's distribution range **(d)** Proportions of suitable niche areas in each landscape under current and future climatic scenarios *(SSP4.5 for 2070/2090 and SSP8.5 for 2070/2090)* **(e)** Resistance surface map showing higher landscape connectivity (green) in the Hengduanshan and Qilianshan landscapes in the northeast compared to reduced connectivity in the Yarlung Zangbo and Western landscapes **(f)** Proportion of heterozygous sites in local Tibetan Partridge populations, indicating reduced heterozygosity in the Western landscape.

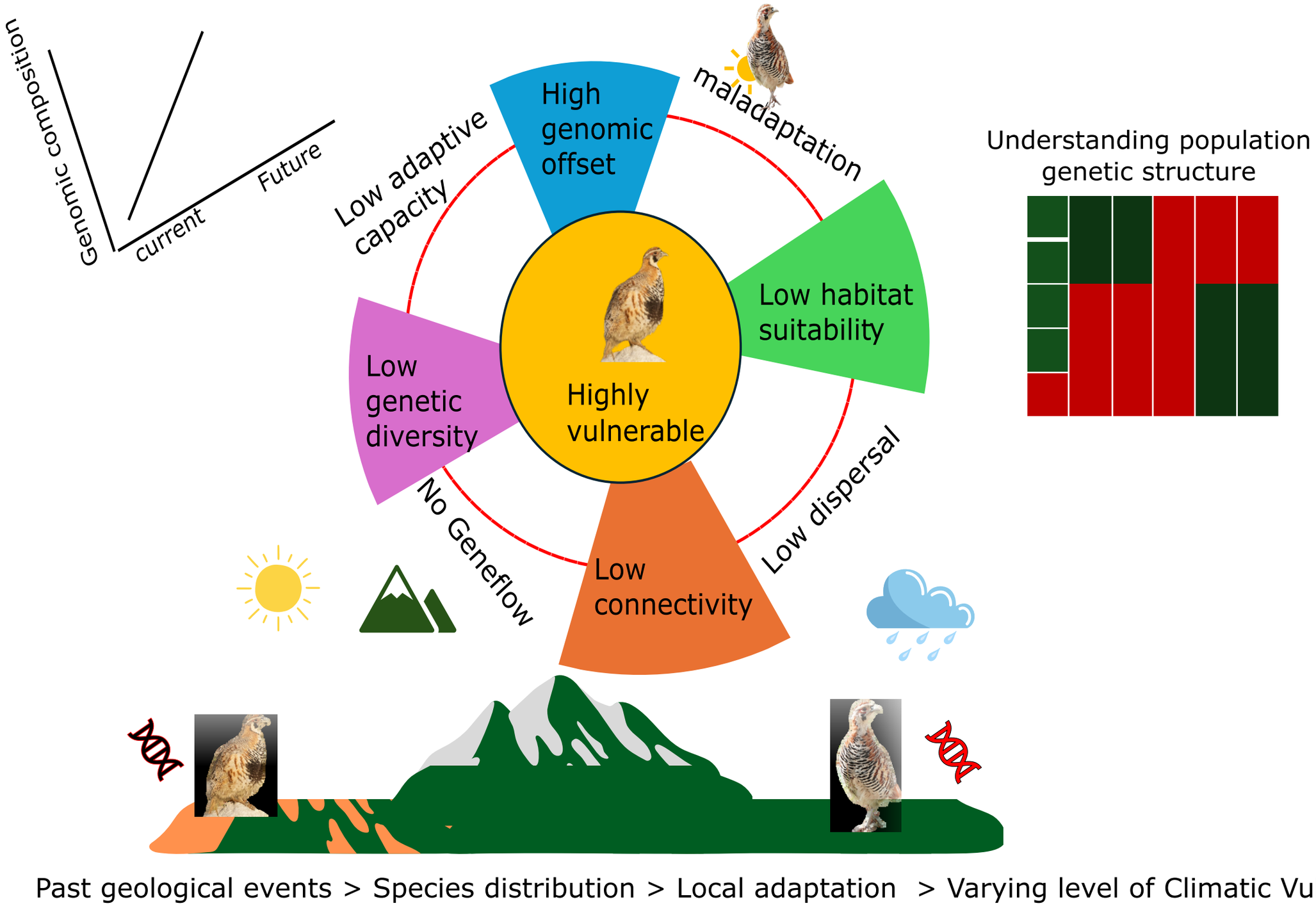

Figure 5: Conceptual framework of using genomic, ecological and landscape information to understand climatic vulnerability. Past geological events shape distribution of species such that formation of barriers and subsequent local adaptation promoting population divergence. These population are exposed to varying level of climatic vulnerability depending upon their genetics, ecology, and landscape connectivity.